Nuclear Engineering and Technology 49 (2017) 277–284

Available online at ScienceDirect

Nuclear Engineering and Technology

journal homepage: www.elsevier.com/locate/net

Technical Note

Neutron Calibration Field of a Bare ^{252}Cf Source in Vietnam

Thiem Ngoc Le [a,*], *Hoai-Nam Tran* [b], *Khai Tuan Nguyen* [a], *and Giap Van Trinh* [a]

[a] *Institute for Nuclear Science and Technology, Vinatom, 179 Hoang Quoc Viet, Hanoi 100000, Viet Nam*
[b] *Institute of Research and Development, Duy Tan University, K7/25 Quang Trung, Da Nang 550000, Viet Nam*

ARTICLE INFO

Article history:
Received 18 April 2016
Received in revised form
12 June 2016
Accepted 30 July 2016
Available online 24 August 2016

Keywords:
^{252}Cf Neutron Source
Neutron Calibration Field
Neutron Flux Spectra
Shadow Cone

ABSTRACT

This paper presents the establishment and characterization of a neutron calibration field using a bare ^{252}Cf source of low neutron source strength in Vietnam. The characterization of the field in terms of neutron flux spectra and neutron ambient dose equivalent rates were performed by Monte Carlo simulations using the MCNP5 code. The anisotropy effect of the source was also investigated. The neutron ambient dose equivalent rates at three reference distances of 75, 125, and 150 cm from the source were calculated and compared with the measurements using the Aloka TPS-451C neutron survey meters. The discrepancy between the calculated and measured values is found to be about 10%. To separate the scattered and the direct components from the total neutron flux spectra, an in-house shadow cone of 10% borated polyethylene was used. The shielding efficiency of the shadow cone was estimated using the MCNP5 code. The results confirmed that the shielding efficiency of the shadow cone is acceptable.

1. Introduction

Together with the national nuclear power program to introduce the first nuclear power plant in Vietnam within the next decade, the increasing use of radiation and neutron sources for research and industrial applications requires a domestic calibration facility for calibrating neutron measuring devices. The Institute for Nuclear Science and Technology (INST), a subinstitute of the Vietnam Atomic Energy Institute, and a member in the International Atomic Energy Agency/World Health Organization secondary standard dosimetry laboratory (SSDL) network [1], possesses a unique SSDL in Vietnam on ionizing radiation dosimetry and calibration. This paper presents the establishment of a neutron detector calibration laboratory at the INST and the characterization of the bare ^{252}Cf spontaneous fission neutron source of low source strength, which was installed at the center of the calibration room.

In general, the total neutron spectrum of the ^{252}Cf source measured by the neutron measuring devices consists of two components: a direct component of neutrons coming to the devices directly from the source without any interaction and a

* *Corresponding author.*
E-mail address: lnthiem@vinatom.gov.vn (T.N. Le).
http://dx.doi.org/10.1016/j.net.2016.07.011

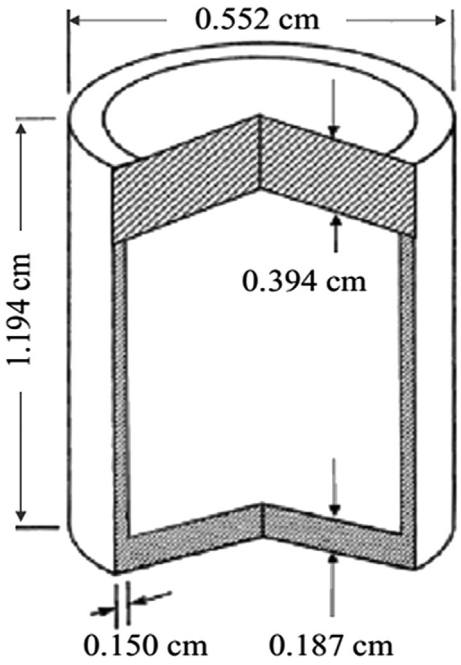

Fig. 1 – The ^{252}Cf neutron source encapsulated by a cylindrical 304L stainless steel cover.

scattered component coming to the devices after interactions with surrounding objects in the calibration room, such as the air and concrete walls. These two components can be separated from the total spectrum using a well-known shadow cone technique. The total neutron component is obtained in measurement without a shadow cone between the source and the detector. The scattered component can be measured by placing the shadow cone of 10% borated polyethylene between the source and the detector to shield the direct component. Then, the direct component of the neutron field is deduced by subtracting the scattered component from the total one. In this work, the total, the scattered, and the direct neutron flux spectra at three reference points of 75, 125, and 150 cm apart from the source were simulated using the MCNP5 code [2]. The corresponding neutron ambient dose equivalent (nDE) rates at the three distances were then calculated by applying the International Commission on Radiological Protection (ICRP) 74 conversion factors [3]. The calculated nDE rates were compared with those measured by Aloka TPS-451C neutron survey meters. In the practical calibration process, the conventional true values of the interested quantities are obtained using a proposed fitting approach. The shielding efficiency of the shadow cone and the anisotropy of the ^{252}Cf neutron source were also estimated.

2. Materials and methods

2.1. ^{252}Cf neutron source and calibration room

A bare ^{252}Cf neutron fission source supplied by Frontier Technology Corporation, Xenia, Ohio, USA was installed at the center of the calibration room. The initial neutron source strength on August 29, 2003 is 1.1×10^7 second^{-1}, as indicated in the supplier's certificate. The source is encapsulated by a cylindrical 304L stainless steel layer with a length of 1.194 cm and an outer diameter of 0.552 cm. The detailed dimensions of the source are shown in Fig. 1. The top view and the side view of the neutron calibration room are displayed in Fig. 2 with the ^{252}Cf neutron source located at the room center. The calibration room has the inner dimensions of $700 \times 700 \times 700$ cm. The concrete wall thicknesses, the position of the source, and the reference point are illustrated in Fig. 2. An aluminum midfloor, consisting of intermittent parallelepiped bars, with a thickness of about 0.2 cm, is installed at a height of 230 cm from the floor base for the detector installation process. This aluminum midfloor does not significantly affect the scattering of neutron because of its low neutron scattering cross section.

In constructing the calibration room and manufacturing the experimental facilities, we followed the international standard guided in the PNNL-15870 Rev. 1 report of Pacific Northwest National Laboratory (PNNL) [4]. However, because the precise qualification of construction and manufacturing

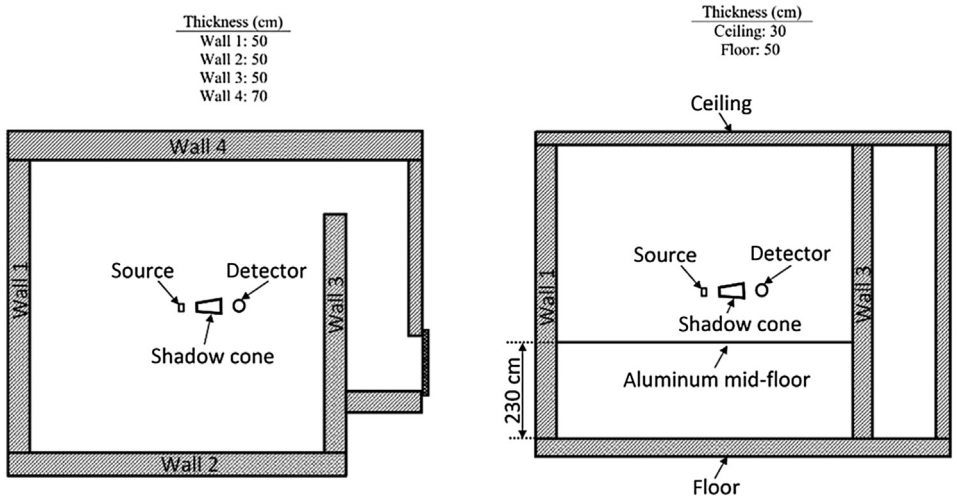

Fig. 2 – Top view (left) and side view (right) of the neutron calibration room.

could not be evaluated, in the numerical simulations using MCNP5, we used the material compositions taken from the PNNL-15870 Rev. 1 report as listed in Table 1 [4]. The discrepancy between the actual material compositions and the data used in the simulation could contribute to the source of uncertainty between the measurements and simulation results, but the uncertainty is expected to be sufficiently small. The interaction cross section data of neutrons were taken from the Evaluated Nuclear Data Files (ENDF/B-VI library) [5]. The ^{252}Cf source was located at the center of the calibration room (120 cm higher than the aluminum midfloor) so that the cylindrical symmetric axis was perpendicular to the floor.

In the simulations, the source was considered as a uniform source with a half-life of 2.65 years. The shielding effect of the source capsulation layer was negligibly small because of the small stainless steel thickness (0.150–0.394 cm). For simplification of the simulation model, it is assumed that the source has a Maxwellian distribution spectrum defined as follows [6]:

$$B_E = \frac{2}{\sqrt{\pi}T^{3/2}} \cdot \sqrt{E} e^{-E/T} B, \quad (1)$$

where B and B_E are the total source strength and the source strength at the energy E, respectively. $T = 1.42$ is the spectrum parameter.

The simulated results of the scattered neutron flux spectra at the three reference distances were obtained using MCNP5 when the shadow cone was located between the source and the reference points. The shadow cone was placed so that its symmetric axis traversing through the reference point was perpendicular to the source central axis at its central point. The smaller base of the shadow cone was placed at 15, 40, and 50 cm from the source center corresponding to the three reference distances, respectively. The F4 tally option of MCNP5 allows scoring average neutron flux in a geometry based on track length estimation [7]. In the simulation, the F4 tally was used to score the total and scattered components in a spherical cell with a radius of 10 cm with the 1–σ standard uncertainties of the integral neutron fluxes within 3% and 1%, respectively. The size of the cell was chosen by considering the common size of neutron detectors. The "Fmesh4" tally was used to calculate the space dependence of the total neutron fluxes in superimposed mesh cells [7]. Cubic finer meshes with a volume of 1 cm^3 were defined to determine the space dependence of the total neutron fluxes (all related objects, except the shadow cone, in the calibration room were included in the input file) with the 1–σ standard uncertainty within 5%. The F5 tally [7] was applied to investigate the shielding efficiency of the shadow cone through the estimation of neutron flux contributions by each cell. In MCNP5 simulations, the numbers of running histories were chosen to assure that the 1–σ standard uncertainties of the integral neutron fluxes as low as acceptable (within 0.5%).

2.2. Instrumentations

Two portable neutron survey meters (Aloka-TPS-451C) were used to measure the nDE rates in the experiments. The neutron survey meter consists of a cylindrical proportional counter 15.5 cm in length and 2.5 cm in diameter filled with 5 atm ^{3}He gas at 20°C, which is covered by a cylindrical moderator of high-density polyethylene ($\rho = 0.95$ g/cm^3) with a length of 23.0 cm and a diameter of 21.0 cm. The counter has cylindrical effective dimensions of 7.0 cm in length and 2.4 cm in diameter. The meters can be used to measure the neutrons in the energy range from 25×10^{-9} to 15 MeV with the neutron ambient dose equivalent rate up to 10 mSv/h. In general, the meter is not sensitive to photons.

Table 1 – Material compositions and weight fractions of the main objects used in the simulations.

Nuclide	Object/material				
	Source case/304L stainless Steel	Wall/ concrete	Calibration room/ air	Shadow cone/borated polyethylene	Midfloor/ aluminum
	8.00[a]	2.35[a]	0.001205[a]	1.00[a]	2.6989[a]
^{1}H	–	0.008485	–	0.125355	–
B	–	–	–	0.100000	–
C	0.000150	0.050064	0.000124	0.774645	–
^{14}N	–	–	0.755268	–	–
^{16}O	–	0.473483	0.231781	–	–
Ar	–	–	0.012827	–	–
Mg	–	0.024183	–	–	–
^{27}Al	–	0.036063	–	–	1.000000
Si	0.005000	0.145100	–	–	–
^{31}P	0.000230	–	–	–	–
S	0.000150	0.002970	–	–	–
K	–	0.001697	–	–	–
Cr	0.190000	–	–	–	–
^{55}Mn	0.010000	–	–	–	–
Ca	–	0.246924	–	–	–
Fe	0.694480	0.011031	–	–	–
Ni	0.100000	–	–	–	–

Note. From Compendium of Material Composition Data for Radiation Transport Modeling, by J. McConn Jr., C.J. Gesh, R.T. Pagh, R.A. Rucker, R.G. Williams III, 2011, PNNL-15870 Rev. 1, Pacific North West National Laboratory, Washington.

[a] Density (g/cm^3).

In the experiments, the neutron survey meters were alternatively placed at the three reference distances, respectively, so that the central axes of the meters were parallel with the floor base and perpendicular to the central beam line at the effective points. The total nDE rates were then measured at three distances without the shadow cone between the source and the meters. The scattered nDE rates were measured by placing the shadow cone between the source and the meters.

In general, an ISO (International Organization for Standardization)-recommended shadow cone consists of two parts: a front end (with a length of 20 cm, made of iron or copper) and a rear section (with a length of 30 cm, made of polyethylene with 5% or more boron) [8]. Because such ISO shadow cone was not available, in this measurement we used an in-house shadow cone consisting of only the polyethylene part with 10% boron. The boron content of 10% is consistent with that suggested for an ISO shadow cone [8]. The iron or copper component is neglected because it is considered that the neutron-induced photon spectra of the ^{252}Cf neutron source were negligibly small—less than 5% during the first 20 years [6]. The shadow cone has a length of 30 cm, with a smaller diameter of 9.0 cm and a larger diameter of 15 cm. Similar shadow cones have also been used effectively in other laboratories to calibrate the ambient dose equivalent meters [9]. In the measurements of the scattered nDE rates at the three reference distances of 75, 125, and 150 cm, the shadow cone was placed such a way that its smaller base was at distances of 15, 40, and 50 cm from the source center, respectively. The geometry of the shadow cone was chosen taking

Table 2 – Total (Φ_{n-tot}) and scattered (Φ_{n-sct}) neutron flux spectra (cm^{-2}/fission/unit lethargy) at the three reference distances.

Energy (MeV)	Neutron flux spectra (cm^{-2}/fission/unit lethargy)					
	75 cm		125 cm		150 cm	
	Φ_{n-tot}	Φ_{n-sct}	Φ_{n-tot}	Φ_{n-sct}	Φ_{n-tot}	Φ_{n-sct}
1.00×10^{-8}	5.70×10^{-8}	5.15×10^{-8}	5.63×10^{-8}	5.50×10^{-8}	5.75×10^{-8}	5.55×10^{-8}
2.53×10^{-8}	2.03×10^{-7}	1.87×10^{-7}	2.12×10^{-7}	1.99×10^{-7}	2.11×10^{-7}	2.02×10^{-7}
1.00×10^{-7}	7.06×10^{-7}	6.39×10^{-7}	7.05×10^{-7}	6.83×10^{-7}	7.06×10^{-7}	6.89×10^{-7}
2.00×10^{-7}	1.48×10^{-7}	1.33×10^{-7}	1.44×10^{-7}	1.42×10^{-7}	1.50×10^{-7}	1.44×10^{-7}
5.00×10^{-7}	6.63×10^{-8}	5.89×10^{-8}	6.57×10^{-8}	6.28×10^{-8}	6.73×10^{-8}	6.48×10^{-8}
1.00×10^{-6}	4.44×10^{-8}	4.02×10^{-8}	4.51×10^{-8}	4.33×10^{-8}	4.30×10^{-8}	4.28×10^{-8}
2.00×10^{-6}	4.38×10^{-8}	4.02×10^{-8}	4.54×10^{-8}	4.28×10^{-8}	4.51×10^{-8}	4.38×10^{-8}
5.00×10^{-6}	5.89×10^{-8}	5.39×10^{-8}	5.59×10^{-8}	5.78×10^{-8}	6.01×10^{-8}	5.80×10^{-8}
1.00×10^{-5}	4.64×10^{-8}	4.20×10^{-8}	4.53×10^{-8}	4.46×10^{-8}	4.69×10^{-8}	4.50×10^{-8}
2.00×10^{-5}	4.69×10^{-8}	4.28×10^{-8}	4.64×10^{-8}	4.50×10^{-8}	4.41×10^{-8}	4.55×10^{-8}
5.00×10^{-5}	6.53×10^{-8}	5.82×10^{-8}	6.06×10^{-8}	6.18×10^{-8}	6.39×10^{-8}	6.20×10^{-8}
1.00×10^{-4}	4.82×10^{-8}	4.54×10^{-8}	4.83×10^{-8}	4.78×10^{-8}	4.70×10^{-8}	4.84×10^{-8}
2.00×10^{-4}	4.98×10^{-8}	4.67×10^{-8}	5.24×10^{-8}	4.86×10^{-8}	5.23×10^{-8}	4.96×10^{-8}
5.00×10^{-4}	6.80×10^{-8}	6.34×10^{-8}	6.84×10^{-8}	6.62×10^{-8}	6.98×10^{-8}	6.71×10^{-8}
1.00×10^{-3}	5.36×10^{-8}	4.94×10^{-8}	5.32×10^{-8}	5.14×10^{-8}	5.49×10^{-8}	5.27×10^{-8}
2.00×10^{-3}	5.67×10^{-8}	5.12×10^{-8}	5.39×10^{-8}	5.33×10^{-8}	5.33×10^{-8}	5.33×10^{-8}
5.00×10^{-3}	7.62×10^{-8}	6.99×10^{-8}	7.52×10^{-8}	7.34×10^{-8}	7.90×10^{-8}	7.43×10^{-8}
1.00×10^{-2}	6.45×10^{-8}	5.53×10^{-8}	6.11×10^{-8}	5.82×10^{-8}	6.16×10^{-8}	5.92×10^{-8}
2.00×10^{-2}	8.15×10^{-8}	5.97×10^{-8}	6.78×10^{-8}	6.22×10^{-8}	6.64×10^{-8}	6.33×10^{-8}
3.00×10^{-2}	5.74×10^{-8}	3.83×10^{-8}	4.52×10^{-8}	4.02×10^{-8}	4.41×10^{-8}	4.07×10^{-8}
5.00×10^{-2}	9.82×10^{-8}	5.25×10^{-8}	7.09×10^{-8}	5.51×10^{-8}	6.81×10^{-8}	5.54×10^{-8}
7.00×10^{-2}	9.15×10^{-8}	3.95×10^{-8}	6.07×10^{-8}	4.14×10^{-8}	5.53×10^{-8}	4.13×10^{-8}
1.00×10^{-1}	1.46×10^{-7}	4.69×10^{-8}	8.25×10^{-8}	4.93×10^{-8}	7.31×10^{-8}	4.93×10^{-8}
1.50×10^{-1}	2.55×10^{-7}	6.57×10^{-8}	1.36×10^{-7}	6.87×10^{-8}	1.17×10^{-7}	6.89×10^{-8}
2.00×10^{-1}	2.62×10^{-7}	5.50×10^{-8}	1.31×10^{-7}	5.85×10^{-8}	1.11×10^{-7}	5.89×10^{-8}
3.00×10^{-1}	5.40×10^{-7}	9.12×10^{-8}	2.55×10^{-7}	9.60×10^{-8}	2.04×10^{-7}	9.61×10^{-8}
5.00×10^{-1}	1.12×10^{-6}	1.15×10^{-7}	4.76×10^{-7}	1.19×10^{-7}	3.68×10^{-7}	1.20×10^{-7}
7.00×10^{-1}	1.16×10^{-6}	1.03×10^{-7}	4.84×10^{-7}	1.08×10^{-7}	3.69×10^{-7}	1.08×10^{-7}
9.00×10^{-1}	1.16×10^{-6}	1.13×10^{-7}	4.94×10^{-7}	1.18×10^{-7}	3.78×10^{-7}	1.17×10^{-7}
1.00×10^{0}	5.41×10^{-7}	3.17×10^{-8}	2.13×10^{-7}	3.20×10^{-8}	1.60×10^{-7}	3.22×10^{-8}
1.20×10^{0}	1.04×10^{-6}	4.92×10^{-8}	4.02×10^{-7}	5.02×10^{-8}	2.97×10^{-7}	5.04×10^{-8}
2.00×10^{0}	3.43×10^{-6}	1.45×10^{-7}	1.33×10^{-6}	1.47×10^{-7}	9.68×10^{-7}	1.47×10^{-7}
3.00×10^{0}	2.83×10^{-6}	1.11×10^{-7}	1.08×10^{-6}	1.08×10^{-7}	7.83×10^{-7}	1.07×10^{-7}
4.00×10^{0}	1.60×10^{-6}	3.28×10^{-8}	5.87×10^{-7}	2.73×10^{-8}	4.13×10^{-7}	2.64×10^{-8}
5.00×10^{0}	8.92×10^{-7}	1.93×10^{-8}	3.31×10^{-7}	1.21×10^{-8}	2.31×10^{-7}	1.14×10^{-8}
6.00×10^{0}	4.89×10^{-7}	1.26×10^{-8}	1.78×10^{-7}	5.79×10^{-9}	1.25×10^{-7}	5.02×10^{-9}
7.00×10^{0}	2.63×10^{-7}	7.89×10^{-9}	9.66×10^{-8}	3.03×10^{-9}	6.74×10^{-8}	2.56×10^{-9}
8.00×10^{0}	1.42×10^{-7}	4.31×10^{-9}	5.08×10^{-8}	1.38×10^{-9}	3.54×10^{-8}	1.13×10^{-9}
9.00×10^{0}	7.27×10^{-8}	2.95×10^{-9}	2.60×10^{-8}	1.05×10^{-9}	1.81×10^{-8}	8.43×10^{-10}
1.00×10^{1}	3.92×10^{-8}	1.70×10^{-9}	1.38×10^{-8}	5.49×10^{-10}	9.33×10^{-9}	3.89×10^{-10}
1.20×10^{1}	3.14×10^{-8}	1.61×10^{-9}	1.18×10^{-8}	4.86×10^{-10}	8.10×10^{-9}	3.48×10^{-10}
1.40×10^{1}	9.01×10^{-9}	5.11×10^{-10}	3.35×10^{-9}	1.40×10^{-10}	2.27×10^{-9}	4.58×10^{-11}

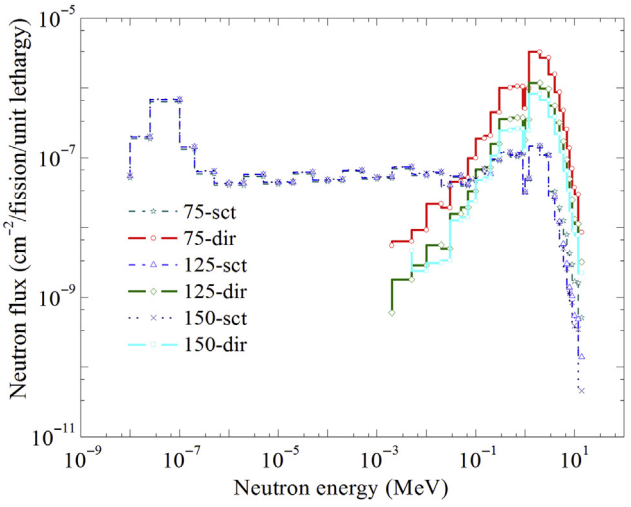

Fig. 3 – Scattered (sct) and direct (dir) neutron flux spectra obtained by MCNP5 simulations at the reference distances of 75, 125, and 150 cm from the source.

into account the ISO recommendations [8]. The shielding efficiency of this shadow cone will also be evaluated and discussed in the next section.

3. Results and discussion

3.1. *Neutron flux spectra and calculation of neutron dose equivalent rate*

Characterization of the neutron flux spectra was based on MCNP5 simulations with existing ICRP 74 energy bins [3]. Table 2 shows the total (denoted as Φ_{n-tot}) and the scattered (denoted as Φ_{n-sct}) components of the neutron flux spectra as a function of energy bins at the three reference distances obtained from MCNP5 calculations. The 1–σ statistical uncertainties of the integral simulated results for Φ_{n-tot} and Φ_{n-sct} were within 3% and 1%, respectively, which were considerably negligible. The direct component of the neutron flux spectra (denoted as Φ_{n-dir}) at the three reference distances are then deduced $(= \Phi_{n-tot} - \Phi_{n-sct})$ with the assumption that the Φ_{n-dir} of the bare ^{252}Cf neutron fission source are at the energy greater than 2.0×10^{-3} MeV [10]. Fig. 3 shows the direct and scattered neutron flux spectra at the three reference distances. It can be seen that the scattered neutron flux spectra in the range of investigated distances are almost unchanged. This gives a certain convenience for the practical calibration to extract the scattered components. Once the neutron flux spectra were obtained, the neutron dose equivalent rates of component p, denoted as nDE_p (μSv/h), were calculated as:

$$nDE_p = \sum_{i=1}^{n} \left[(\Phi_{n-p})_i \times (h_\Phi)_i \right] \times A_s, \quad (2)$$

where p = (tot, sct, dir) refers to the total, scattered, or direct component of the neutron spectrum; A_s is the total neutron source strength (s^{-1}); Φ_{n-p} is the neutron flux of component p; and $(h_\Phi)_i$ is the conversion factor from unit neutron flux to neutron ambient dose equivalent in the ith energy bin [3,11]. Taking into account the total neutron source strength on the date of measurement (December 22, 2014) of 568,997 second^{-1} and the calculated neutron fluxes given in Table 2 accompanied with the appropriate conversion factors, the nDE_p rates were calculated as shown in Table 3. The measured nDE_p rates at the three distances using the two neutron survey meters are also summarized in Table 3 together with the corresponding statistical uncertainties. In the present work, each measurement was repeated 10 times at each point with each survey meter to obtain the mean values of the neutron dose equivalent rates and the statistical uncertainties.

3.2. *Fitting of the measured total neutron dose equivalent rates and the simulated total neutron flux*

According to the ISO recommendation [8], the nDE_{tot} rates obtained by experiments can be expressed as follows:

$$(nDE_{tot} - nDE_{sct}) \times F_A(d) = k \times d^{-2}, \quad (3)$$

where $F_A(d)$ is the appropriate air attenuation (air out-scatter) factor, k is the characteristic constant, and d is the distance from the source to the reference point. The nDE_{sct} rate is considered constant in the range of the investigated distances

Table 3 – Neutron ambient dose equivalent rates at the three reference distances obtained from simulation, fitting and measurement by the AlokaTPS-451G meter.

Distance (cm)	Method	Neutron ambient dose equivalent rate (μSv/hr)			
		Total	Scattered	Direct[a]	Direct[b]
75	Simulated	12.8	0.75	12.1	12.6
	Meter 1	11.85 ± 1.03	0.82 ± 0.10	11.03 ± 1.03	11.40
	Meter 2	12.17 ± 1.00	0.85 ± 0.09	11.32 ± 1.00	
125	Simulated	5.04	0.74	4.30	4.54
	Meter 1	4.61 ± 0.36	0.78 ± 0.11	3.83 ± 0.37	4.10
	Meter 2	4.79 ± 0.33	0.82 ± 0.06	3.97 ± 0.33	
150	Simulated	3.73	0.74	2.99	3.15
	Meter 1	3.49 ± 0.23	0.68 ± 0.05	2.81 ± 0.23	2.85
	Meter 2	3.44 ± 0.19	0.70 ± 0.07	2.74 ± 0.20	

[a] Total—scattered.
[b] Calculated according to Eqs. (5) and (7) for the measured and simulated neutron dose equivalent rates, respectively.

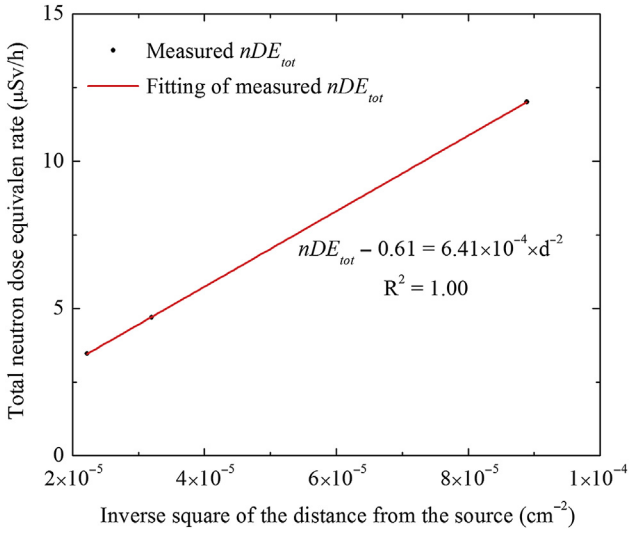

Fig. 4 – The total neutron dose equivalent (nDE_{tot}) rate measured by neutron survey meters as a function of the inverse square of the distance from the source.

as shown in Fig. 3. If the air attenuation factor, $F_A(d) = \exp[-d\cdot\sum]$ (where $\sum$ is the average linear attenuation coefficient, which is equal to 1,055 × 10^{-7} cm^{-1} for the bare ^{252}Cf neutron source [8]), is negligible compared to the room scattering factor (in most practical cases), then Eq. (3) can be rewritten as:

$$nDE_{tot} - nDE_{sct} = k \times d^{-2} \quad (4)$$

The nDE_{tot} rates measured by neutron survey meters were then fitted as a function of the inverse of square distances from the source according to Eq. (4), and the result is illustrated in Fig. 4. Combining the fitting equation in Fig. 4 and Eq. (4), one can see that the nDE_{sct} rate is constant at 0.61 (μSv/h), and the direct component nDE_{dir} can be expressed as:

$$nDE_{dir} = 6.41 \times 10^{-4} \times d^{-2} \quad (5)$$

Fig. 5 displays the contour plot of the total neutron fluxes obtained from the MCNP5 simulation on the plane perpendicular to the source axis at its central point. This figure can be useful for checking the neutron flux measured by the devices and for understanding the distribution of the neutron fluxes in the calibration room. The total component Φ_{n-tot} can also be fitted according to Eq. (4), and the correlation is displayed in Fig. 6. As a result, the Φ_{n-dir} (cm^{-2}/fission/unit lethargy) and the nDE_{dir} rate can be expressed by Eqs. (6) and (7), respectively, where h_Φ is 385 pSv cm^2 for the ^{252}Cf source. The calculated nDE_{dir} at three different reference distances through Eq. (7) are also shown in Table 3.

$$\Phi_{n-dir} = 0.09 \times d^{-2} \quad (6)$$

$$nDE_{dir} = \Phi_{n-dir} \times h_\Phi \times A_s \quad (7)$$

The results in this section illustrate that the proposed fitting approach can be practically applied to calculate the conventional true value of the ambient dose equivalent rate for the purpose of calibrating neutron survey meters.

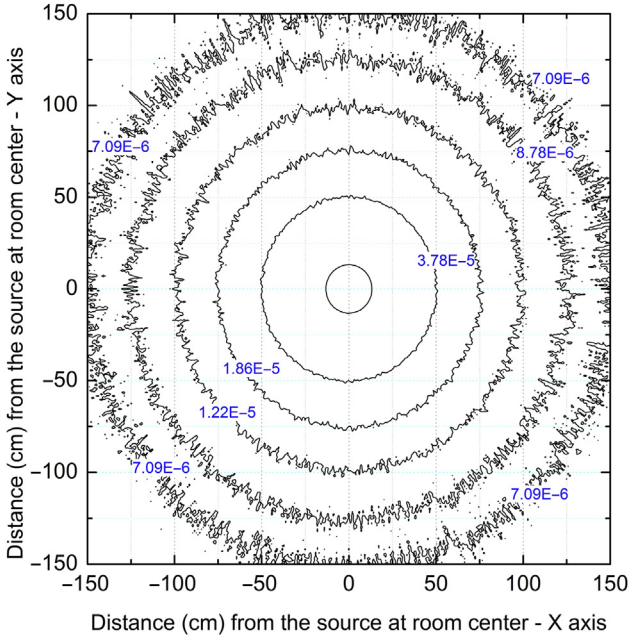

Fig. 5 – Contour plot of the total neutron flux (cm^{-2}/fission/unit lethargy) on the central plane of the calibration room.

3.3. *Anisotropy of the source*

The anisotropy of the ^{252}Cf neutron source was calculated using MCNP5 with the "Fmesh4" tally [7]. The cylinder with a radius of 150 cm and a height equal to the source diameter, which has the central point at the source center and its central axis is perpendicular to that of the source, was divided into equal sectorial meshes with a solid angle of $\pi/19$. MCNP5 input files with "Fmesh4" tally were compiled to calculate the angular neutron source strength (i.e., neutron flux in each mesh lattice). Then, the angular source strength at the angle of $\pi/2$ was normalized to the average source strength to calculate the anisotropy of the source. The anisotropic correction factor of 1.013 at the angle of $\pi/2$ was observed, which is negligible for the ^{252}Cf neutron source used in the experiments.

3.4. *Shielding efficiency of the shadow cone*

As the neutron-induced photon flux spectra of the ^{252}Cf source were negligibly small [6], the shadow cone of a polyethylene component of 10% boron was used in the measurements of the scattering component. The shielding efficiency of this shadow cone was investigated by comparing the penetrating neutron flux (the contribution of the source) to the overall scattered neutron flux obtained from MCNP5 simulation at the reference distance of 75 cm. Fig. 7 shows the detailed contributions of the main objects in the calibration room to the overall scattered neuron flux. One can see that the contribution of the source and the source cover to the overall scattered neutron flux is about 0.43%, which is considered negligibly small. This means that the cone shielding efficiency is

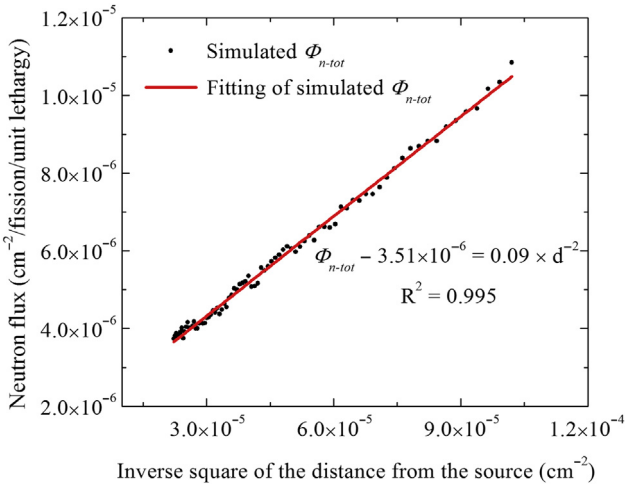

Fig. 6 – Total neutron flux (Φ_{n-tot}) simulated by MCNP5 code as a function of inverse square of the distance from the source.

sufficient for the purpose of shielding the direct neutron component. In other words, the use of this shadow cone is practically acceptable.

3.5. *Comparison of simulation and measurement*

Comparing the nDE_{dir} rates obtained from the MCNP5 simulations (in Eq. (7)) to the measured values and the values obtained from the fitting curves, the discrepancy of about 10% between the simulation and measurement results is achieved as shown in Table 3, which is considerably acceptable. The discrepancy is ascribed to the following sources of uncertainties: from the MCNP5 simulations, the fitting approach, and the experiments.

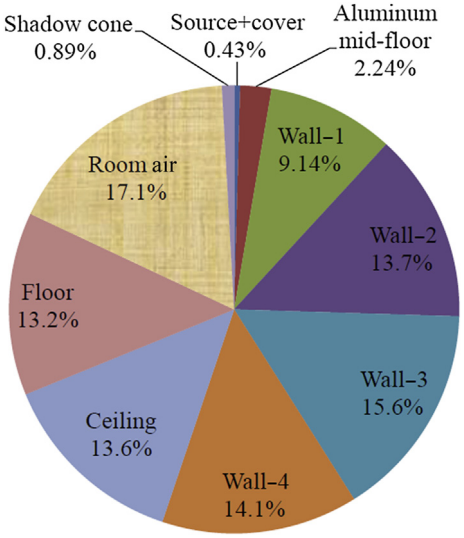

Fig. 7 – Neutron flux contributions of the main objects in the calibration room to the overall scattered neutron flux at the reference distance of 75 cm. The concrete walls are numbered as in Fig. 2.

The standard uncertainties of the simulated nDE rates are affected by all factors in Eq. (2) (i.e., uncertainties of the total source strength, the simulated neutron flux, and the conversion factor), which are, unfortunately, not fully available; thus, these standard uncertainties are difficult to evaluate. However, the statistical uncertainties of the simulated nDE rates are mainly affected by the uncertainties of the integral simulated neutron fluxes, which are reasonably assumed to be as low as negligible. According to Eqs. (5) and (7), the uncertainties of fitting curves are affected by the uncertainties of the slope factors of the fitting curves, but the uncertainties of the fitting curves are acceptable in this case because the square of the correlation factor R is close to unity. In the measurement, the statistical uncertainties of the measured nDE rates are normally reduced by repeating the measurement a number of times. Although this condition was performed in the experiments, the statistical uncertainties of the measured nDE rates was about 10% (see Table 3).

The discrepancy of about 10% among the nDE rates, as shown in Table 3, is considerably acceptable for the purpose of radiation protection at low levels of neuron ambient dose equivalent rates. The agreement between the simulated and measured nDE rates implies that the neutron energy response function of Aloka TPS-451C neutron survey meter complies with the ICRP 74 conversion factor function. The characteristics are consistent with the meter manufacturer's statement [12].

4. Conclusion

The first neutron calibration field of a bare ^{252}Cf source was established in Vietnam. The characterization of the neutron calibration field in terms of neutron flux spectra was based on the Monte Carlo simulations using the MCNP5 code. Neutron ambient dose equivalent rates at the three reference distances of 75, 125, and 150 cm from the source were calculated and compared with the measured values. The results show that the discrepancy between the calculated and measured values is about 10%.

A shadow cone of 10% borated polyethylene was successfully applied to shield the direct component of the neutron flux spectra for the low photon contaminated ^{252}Cf neutron source. The simulated results show that the cone shielding efficiency meets the ISO 8529-2:2000 criteria. The anisotropy correction factor of the ^{252}Cf neutron source was negligible. As the scattered neutron flux spectra in the investigated distances from the source to the reference points are almost constant, a fitting approach is proposed and applied for predicting the conventional true value of quantities of interest for the purpose of neutron survey meter calibration.

Conflict of interest

All authors have no conflicts of interest to declare.

Acknowledgments

The authors are grateful to Dr Pham Ngoc Diep of Vietnam National Satellite Center for valuable discussions. Mr Vu

Manh Khoi, Mr Ho Quang Tuan, and Dr Nguyen Thanh Tuy of INST are also greatly acknowledged for their kind assistance and support during the experiments.

REFERENCES

[1] The IAEA/WHO SSDL Network. http://www-naweb.iaea.org/nahu/dmrp/SSDL/login.asp, (accessed on 15.04.16).
[2] X-5 Monte Carlo Team, MCNP—A General Monte Carlo N-particle Transport Code, Version 5, vol. I: Overview and Theory, Los Alamos National Laboratory, California, 2003, p. 334.
[3] ICRP Publication 74, Conversion coefficients for use in radiological protection against external Radiation, Ann. ICRP 26 (1996) 3–4.
[4] J. McConn Jr., C.J. Gesh, R.T. Pagh, R.A. Rucker, R.G. Williams III, Compendium of Material Composition Data for Radiation Transport Modeling, PNNL-15870 Rev. 1, Pacific North West National Laboratory, Washington, 2011, p. 375.
[5] P.F. Rose, ENDF-201, ENDF/B-VI Summary Documentation. BNL-NCS-17541, fourth ed., 1991.
[6] ISO 8529-1:2001 (E), Reference Neutron Radiations – Part 1: Characteristics and Methods of Production, ISO, Switzerland, 2001, p. 32.
[7] X-5 Monte Carlo Team, MCNP-A General Monte Carlo N-particle Transport Code, Version 5, vol. II: User's Guide, Los Alamos National Laboratory, California, 2003—Revised 2005, p. 504.
[8] ISO 8529-2:2001 (E), Reference Neutron Radiations – Part 2: Calibration Fundamentals of Radiation Protection Devices Related to the Basic Quantities Characterizing the Radiation Field, ISO, Switzerland, 2000, p. 38.
[9] H. Park, J.H. Kim, D. Webb, V. Sathian, J.H. Lee, Z. Hui, H. Harano, A. Masuda, T. Matsumoto, N.N. Moisseev, A.V. Didyk, APMP comparison for the calibration of ambient dose equivalent meters in ISO neutron reference fields — APMP.RI(III)-S1, Metrologia 52 (2015). Technology Supplement 06019.
[10] IAEA Technical Reports Series, Compendium of Neutron Spectra and Detector Responses for Radiation Protection Purposes — Supplement to Technical Reports Series No. 318. No. 403, 2001, p. 276.
[11] IAEA Safety Standards Series, Assessment of Occupational Exposure Due to External Sources of Radiation. No. RS-G-1.3, 1999, p. 98.
[12] Neutron Survey Meter TPS-451C. http://www.hitachi.com/businesses/healthcare/products-support/radiation/surveymeter/tps451c/index.html, (accessed on 15.04.16).